PROCEEDINGS

SPIE Volume 868

Optoelectronic Technologies for Remote Sensing from Space

John S. Seeley, Stuart C. Bowyer
Chairs/Editors

Organized by
Europtica-Services I.C.
SPIE—The International Society for Optical Engineering

19-20 November 1987
Cannes, France

Proceedings

SPIE Volume 868

Optoelectronic Technologies for Remote Sensing from Space

John S. Seeley, Stuart C. Bowyer
Chairs/Editors

Organized by
Europtica-Services I.C.
SPIE—The International Society for Optical Engineering

19-20 November 1987
Cannes, France

Published and Distributed Worldwide by
SPIE—The International Society for Optical Engineering
P.O. Box 10, Bellingham, Washington 98227-0010 USA
Telephone 206/676-3290 (Pacific Time) • Telex 46-7053

SPIE (The Society of Photo-Optical Instrumentation Engineers) is a nonprofit society dedicated to advancing engineering and scientific applications of optical, electro-optical, and optoelectronic instrumentation, systems, and technology.

The papers appearing in this book comprise the proceedings of the meeting mentioned on the cover and title page. They reflect the authors' opinions and are published as presented and without change, in the interests of timely dissemination. Their inclusion in this publication does not necessarily constitute endorsement by the editors or by SPIE.

Please use the following format to cite material from this book:
Author(s), "Title of Paper," *Optoelectronic Technologies for Remote Sensing from Space,* John S. Seeley, Stuart C. Bowyer, Editors, Proc. SPIE 868, page numbers (1988).

Library of Congress Catalog Card No. 87-63515
ISBN 0-89252-903-2

Printed in the United States of America.

Conference 868, Optoelectronic Technologies for Remote Sensing from Space, was one of nine technical conferences at the

International Symposium on the Technologies for Optoelectronics

16–20 November 1987 • Palais des Festivals et des Congrès • Cannes, France

Cooperating Sponsors

ANRT—Association Nationale de la Recherche Technique
Associazione Elettrotecnica ed Elettronica Italiana
Austrian Physical Society
Battelle-Geneva Research Centres
Comité Belge d'Optique
DGaO—Deutsche Gesellschaft für angewandte Optik
Israel Laser and Electro-Optics Society
Optics Division/Portuguese Physical Society
Promoptica
SEE—Société Française des Electriciens, des Electroniciens et des Radioélectriciens
SGOEM—Schweizerische Gesellschaft für Optik und Elektronenmikroskopie
Sira Ltd.—The Research Association for Instrumentation
Société Française d'Optique
SPIE—The International Society for Optical Engineering

in collaboration with the
Optics Division of the European Physical Society

Technical Organizing Committee

Alfred R. Adams (UK)
Charles E. Barnes (USA)
Jean Besson (France)
Manfred Bohner (FRG)
Gilbert Boisdé (France)
R. C. Booth (UK)
Stuart Bowyer (USA)
Alain Brenac (France)
Jean Bulabois (France)
Sandro Carnevale (Italy)
Jean-Pierre Chatard (France)
Paul Cruvellier (France)
Gottfried H. Döhler (FRG)
Jean Pierre Dumas (France)
William F. Fagan (UK)
Aaron Gara (USA)
Vittorio Ghergia (Italy)
S. Gratze (UK)
P. D. Greene (UK)
Roger A. Greenwell (USA)
Rudolf Grosskopf (FRG)
Jean Pierre Huignard (France)
Graham T. Jenkin (UK)
Richard Johnson (UK)
Werner Jüptner (FRG)
Ralf Th. Kërsten (FRG)
Ralph Kihlén (Sweden)
John W. Lear (USA)
Christian Liegeois (France)
Helmut Loss (FRG)
Horst Maier (FRG)
Fenner Milton (USA)
Antoine Mizzi (France)
A. F. M. Moorwood (FRG)
Masayoshi Murata (Japan)
D. B. Ostrowsky (France)
R. J. Parker (UK)
C. R. Petts (UK)
Roy F. Potter (USA)
Ryszard J. Pryputniewicz (USA)
Claude Puech (France)
Giancarlo C. Righini (Italy)
Roger Samy (France)
John S. Seeley (UK)
Bernard Sermage (France)
Andrew C. Sleigh (UK)
Paul Smigielski (France)
Oliverio D. D. Soares (Portugal)
W. Sohler (FRG)
Erich Spitz (France)
Jean Taboury (France)
Andrew G. Tescher (USA)
Guy Y. Turquet de Beauregard (France)
J. Vleggaar (Netherlands)
Richard Wade (UK)
William L. Wolfe (USA)
M. Yamanishi (Japan)
Hajime Yamashita (Japan)

OPTOELECTRONIC TECHNOLOGIES FOR REMOTE SENSING FROM SPACE

SPIE Volume 868

Conference Committee

Chairs
John S. Seeley
University of Reading (UK)

Stuart C. Bowyer
University of California/Berkeley (USA)

Cochairs
John W. Lear
Grumman Aerospace Corporation (USA)

Paul Cruvellier
CNRS Marseille (France)

Antoine Mizzi
CNES Toulouse (France)

Session Chairs
Session 1—Ultraviolet Technology
Paul Cruvellier, CNRS Marseille (France)

Session 2—Infrared Technology
John S. Seeley, University of Reading (UK)

Session 3—Astronomy
John W. Lear, Grumman Aerospace Corporation (USA)

Session 4—Remote Sensing
Stuart C. Bowyer, University of California/Berkeley (USA)

INTRODUCTION

This conference was the third in a series conducted in Europe on instrumentation for remote sensing. Its predecessors were *Instrumentation for Optical Remote Sensing from Space,* Proc. SPIE 589, Cannes, 1985 (J. S. Seeley, J. W. Lear, A. Monfils, and S. L. Russak, eds.) and *Optical Systems for Space Applications,* Proc. SPIE 810, The Hague, 1987 (H. Lutz and G. Otrio, eds.). One conference on *Earth Remote Sensing Using the Landsat Thematic Mapper and SPOT Sensor Systems,* Proc.SPIE 660, Innsbruck,1986 (P. N. Slater, ed.) has also been held.

As was true previously in Cannes, this conference was structured to indicate long-term continuity and development in optoelectronic technology for the acquisition, detection, and processing of information about our planets and their atmospheres and about astronomical objects. It was a specialty programme emphasising ultraviolet surveillance and atmospheric sensing, infrared atmospheric sensing and imaging, and possibilities for laser sensing. All sessions contained contributions on advanced detector arrays being developed for the appropriate wavelength regions.

As previously, the contributors came from several countries and, on this occasion, multinational projects were described. Thus, the Besançon (French) built spectrometer flown on the Vega 2 (Russian) mission to Halley's comet was highlighted, as were Matra (French) optics intended for the remote sensing satellite of India. The ultraviolet detection systems of the University of California/Berkeley (United States), developed for upper atmosphere exploration, prove relevant for space astronomical telescopes also. The ROSIS of MBB (German) is a surface-imaging candidate for the supposed Polar Platform (ESA/NASA); second generation Meteosat intentions described by Matra (French) relate back to the earliest of international remote sensors, and so on.

Thus, although the constituent sections in the proceedings are entitled Ultraviolet Technology, Infrared Technology, Astronomy, and Remote Sensing, much overlap is to be found among them. The discussions that ensued after most papers were satisfactory to the extent that a scheduled Open Session would have been superfluous and did not take place, although, regrettably, there is no record.

We thank the organisers for their continuing support of this topic and the session chairs, speakers, and attendees for their significant contributions to a stimulating conference. It is hoped that there will be future opportunities to continue the series.

John S. Seeley
University of Reading (UK)

Stuart C. Bowyer
University of California/Berkeley (USA)

OPTOELECTRONIC TECHNOLOGIES FOR REMOTE SENSING FROM SPACE

SPIE Volume 868

Contents

Session 1

Ultraviolet Technology

Chair
Paul Cruvellier
CNRS Marseille (France)

Ultraviolet Surveillance of Boosters and Post-Boost Vehicles

Stuart Bowyer and Mark Hurwitz

Space Sciences Lab, University of California, Berkeley

Abstract

A priority in the Strategic Defense Initiative (SDI) is development of a space-based system to detect, identify, and track ICBMs. We show that ultraviolet surveillance provides advantages unavailable in any other wavelength band. During boost phase it should be possible to identify vehicles by their UV emissions and to track the hard body by detection of the vacuum core. After burn out, UV emission from shocked gas at the vehicle tip may be detectable. This is particularly important for surveillance of "fast burn" boosters, which burn out at a low altitude and hence are virtually invisible to infrared sensors by the time they reach an altitude where the atmosphere is transparent to IR radiation. We discuss the feasibility of tracking conventional and fast-burn vehicles via UV surveillance from space. Estimates of the UV brightness of typical targets are provided. We also consider the ambient day and night time background and evaluate the signal to noise ratio achievable under various viewing scenarios. We discuss instrumentation which should be capable of detecting and tracking such targets from geosynchronous orbit. An added advantage of UV surveillance is the availability of sensitive, rugged UV detectors which are under development by both the U.S. and the U.S.S.R.

Introduction

Historically, the general consensus has been that space-based surveillance at infrared wavelengths represents the best method to detect and track intercontinental ballistic missiles (ICBMs). Although conventional liquid fuel boosters (hereafter LFBs) emit copious IR radiation for the first ~200 seconds of flight and burn out at the relatively high altitude of ~275 km, so called "fast-burn boosters" are specifically designed to thwart IR detection by burning out quickly (~50 sec) and at low altitudes (~80 km) where the residual atmosphere above the vehicle is opaque to IR wavelengths.[1] Even for conventional LFBs the exhaust plume is very extended, making location of the hard body difficult to determine precisely.

Surveillance at ultraviolet wavelengths may be the best method to detect and track LFBs and FBBs. Estimates of the UV brightness of these targets indicate that they may be readily detectable with instruments of modest aperture. Additionally, the background signal from the earth is much fainter at UV than at IR wavelengths. Furthermore the UV emission region is generally small, facilitating location of the hard body itself. In the sections that follow we examine questions of target brightness and background contamination, and suggest instrumentation appropriate for UV surveillance from space.

Target Brightness

Much of the early work in determining the emission from shocked gas was performed in the 1960s as part of the broader task of estimating the heating of re-entry vehicles. By scaling the results of Biberman *et al.*[2] the power radiated at UV wavelengths from the shock at the nose of a fast-burn booster has been estimated to be 0.1 Watts between 2000 and 3000 Å. The size of the shocked region is only a few tens of centimeters in diameter and would probably be unresolved, so at a distance d (km) the UV flux from the shock is given by

$$F_{FBB,\ photons\ \mathrm{cm^{-2}\ sec^{-1}}} = \frac{10^6}{d_{\mathrm{km}}{}^2} \tag{1}$$

where the cm^{-2} subscript on F refers to the effective area of the detecting device. Because of limited work carried out to date it is difficult to predict the relative strengths of the various emission lines and continuum processes that will contribute to the total flux.

Studies of the UV emission from the plume of a conventional LFB suggest that most of the emission comes from the "vacuum core" of the plume, a region approximately 5 × 10 meters in size. An estimate of the total power emitted between 2000 and 3000 Å is 0.25 to 20 watts, although recent experimental results have indicated a surprisingly higher UV power. In order for the instrument to resolve the core, the product of the resolution θ (arcsec) and d_{km} must be less than 1000. If resolved, the flux from the plume core per resolution element will be

$$F_{LFB,\ photons\ \mathrm{cm^{-2}\ sec^{-1}}} = (\ 1.25\ -\ 100\ )\ \theta''^{2} \tag{2}$$

The rationale for resolving the core is to provide additional information to distinguish between the various launch vehicles that might be observed and to locate more accurately the position of the hard body.

The UV Earth Brightness (Down-looking)

A great advantage of UV over IR surveillance is the relative faintness of the earth's background signal. During daytime hours the 2000 - 3000 Å background is primarily continuum radiation with an intensity of ~8000 Rayleighs $Å^{-1}$; at night the background consists of emission lines of NO and O_2 with an integrated intensity of ~150 Rayleighs.[3] For detection of a target producing emission at discrete wavelengths, the signal to noise could be maximized by judicious selection of narrow bandpass filters; however, for the remainder of this work we will assume that the entire 2000 - 3000 Å band is utilized. If the instrument used to perform the observation has a resolution element θ (arcsec), the flux per resolution element due to background is given by

$$F_{day,\ photons\ \mathrm{cm^{-2}\ sec^{-1}}} = 32\ \theta''^{2} \tag{3}$$

$$F_{night,\ photons\ \mathrm{cm^{-2}\ sec^{-1}}} = 3\times10^{-4}\ \theta''^{2} \tag{4}$$

The background rate per resolution element due to non-photon events ("dark counts") is dependent on the physical size of the resolution element on the detector surface which is determined by θ and the focal length of the instrument *f*. For typical values of *f* and θ the dark count rate of microchannel plate (MCP) detectors is orders of magnitude less than the down-looking night time background.

Viewing Scenarios and Instrumentation

For an instrument with a fixed number of detector pixels in the focal plane, there is a direct trade-off between the size of the resolution element θ and the total field of view of the instrument. Today's UV photon counting MCP detectors have formats approaching 1024 × 1024 pixels, which corresponds to 512 × 512 resolution elements assuming 2 detector pixels per (linear) resolution element. Combined with the requirement that the instrument should resolve the core of the plume, the size of the field of view is given by

$$FOV^{\circ} = \frac{142}{d_{\mathrm{km}}} \tag{5}$$

As an example, if the observing distance is 500 km the field of view is restricted to ~17′ . The resolution element in this case is ~2 ″. If the instrument had an adjustable focal length the field of view could be made much larger than that given by equation (5), and some sort of "zoom" system used to achieve high angular resolution after initial detection of the vehicle.

The sensitivity of a UV telescope is straightforward to estimate. Reflective coatings at these wavelengths typically reflect better than 85% of the incident radiation. The filter used to define the bandpass would transmit ~50%, and the detector photocathode would have a quantum efficiency of ~20%. Combining these factors for a two-reflection system with primary aperture radius R_{cm} yields an effective area

$$A_{eff,\ \mathrm{cm^2}} = 0.23\ R_{\mathrm{cm}}^{2}. \tag{6}$$

Signal to Noise from Low Earth Orbit

We calculate the signal to noise ratio for day and night observations of FBBs and LFBs assuming an observing distance of 500 km and a modest telescope aperture *R* of 50 cm. The S/N ratio is also a function of the observation time, which depends in turn on factors such as the target velocity perpendicular to the line of sight and the slew rate of the telescope. Any calculation of the allowable observing time would therefore be highly scenario-specific. As an example we choose an arbitrary observation time of 1 second and present the resulting S/N ratios in Table 1.

TABLE 1:
S/N From Low Earth Orbit

	FBB	LFB (per pixel)
Day	8.5	11 to 850
Night	2800	3500 to 280000

Prospects for Geosynchronous Surveillance

From geosynchronous orbit, the angular resolution θ required to image the vacuum core of an LFB is 0.024″. This represents a challenging goal for conventional optical techniques. Alternatively one could distinguish between the various vehicles by spectral or broadband photometric measurements once the emission mechanisms of LFBs and FBBs are characterized. To estimate the signal to noise achievable from geosynchronous orbit we assume a resolution of 0.1 ″(a realistic goal) and an aperture radius of 100 cm. We present the resulting S/N ratios in Table 2 assuming an integration time of 1 second. Note that in this case the values stated for the LFB refer to the integrated flux from the plume, which would be unresolved with θ = 0.1 ″.

TABLE 2:
S/N From Geosynchronous Orbit

	FBB	LFB
Day	0.5	.12 to 9.3
Night	15	39 to 3000

The S/N ratio could be improved substantially by using pattern recognition techniques (e.g., searching for "streaks") rather than simply relying on detection of UV "flashes" as assumed in our analysis.

Detector Technology

A major concern in any space-based surveillance system is the ruggedness and reliability of the detector unit. For UV wavelengths, flight-qualified photon counting detectors based on microchannel plate stacks are available. Active research programs in the U.S. and U.S.S.R. have produced detectors which are electrically simple, compact, extremely rugged, and operate at ambient temperature. Further information can be found in western[4] and Soviet journals[5]. These detectors have been used in a substantial number of flight instruments[6,7,8] and are baselined for use in the Extreme Ultraviolet Explorer satellite[9]. A comparison of these detectors and CCDs at far UV wavelengths is presented in this conference session[10]. The conclusion of this study is that the performance of MCP detectors is superior in virtually every application. For very high resolution work, a new system of decoding the position of incoming photons is under development by Lampton at the Space Sciences Laboratory at U.C. Berkeley[11].

Conclusions

We have shown that ultraviolet surveillance of conventional liquid fuel boosters and post-burnout "fast burn" vehicles is a promising technique. With a 1 meter diameter telescope in low earth orbit high signal to noise ratios can be achieved in extremely short integration times. From geosynchronous orbit reliable surveillance will require larger apertures and/or pattern recognition software. Additional work, especially imaging and spectroscopy of actual vehicles from space-based telescopes is needed to characterize the various emission mechanisms from these vehicles and better determine the total power radiated in the UV bandpass.

References

1. Velikhov, Y., Sagdeev, R., Kokoshin, A., *Weaponry in Space: The Dilemma of Security,* Mir Publishers, 1986.
2. Biberman, L., Vorobev, V., Norman, G., and Iakubov, I., "Radiation heating in hypersonic flow" *Kosmich Issled*, **2**, 441, 1964.
3. R.E. Huffman, private communication.
4. M. Lampton, "The Microchannel Image Intensifier, *Scientific American* **245**, No. 5, 62, 1981.
5. M. Gruntman, *Journal of Experimental and Theoretical Physics of the U.S.S.R.* (Translated by Plenum Publishers Co.), 1982.
6. C. Martin and S. Bowyer, "Observations of Local Interstellar Medium Emission with the Berkeley EUV/FUV Shuttle Telescope," *Proc. IAU Colloquium 81*, NASA Conference Publication **2345**, 344, 1984.
7. S. Labov, S. Bowyer and C. Martin, "A spectrometer to measure the diffuse, astronomical extreme ultraviolet background," *Proc. SPIE*, **627**, 379, 1986.
8. O.H.W. Siegmund, M. Lampton, J. Bixler, J. Vallerga and S. Bowyer, "High Efficiency Photon Counting Detectors for FAUST FUV Astronomy Payload," *IEEE Trans. Nucl. Sci.*, **NS-34**, No. 1, 1987.
9. R.F. Malina, S. Bowyer, M. Lampton, D. Finley, F. Paresce, G. Penegor and H. Heetderks, "The Extreme Ultraviolet Explorer," *Opt. Eng.*, **21**, 764, 1982.
10. J.V. Vallerga and M. Lampton, "Charge Coupled Devices vs. Microchannel plates in the Extreme and Far Ultraviolet: A Comparison Based on the Latest Laboratory Measurements," *Proc. SPIE*, this conference, 1987.
11. M. Lampton, "Readout Techniques for Photon-Counting Microchannel Image Systems," *Proc. SPIE*, this conference, 1987.

Ionospheric and Atmospheric Remote Sensing Using Passive Sensors

Supriya Chakrabarti, Richard Link and G. Randall Gladstone
Space Sciences Laboratory
University of California
Berkeley, CA 94720

Abstract

Knowledge of the instantaneous state of the ionosphere can facilitate many components of C^3I systems. Traditionally, ionospheric measurements have been performed using Langmuir probes, ion mass spectrometers, radars and ionosondes. The first two sample the ionosphere *in situ*, along the rocket or satellite trajectories. Besides being an active probing method, ground-based radio observations are limited to a geographically fixed area surrounding the measurement site. In recent years it has been shown that ionospheric density distributions can be obtained by the remote sensing of selected Extreme Ultraviolet (EUV) emissions. The sensors for these measurements employ space-based passive detection techniques. The spectral region below 2000 Å has successfully been used to both probe the upper atmosphere and image the aurora, even under fully sunlit conditions. The EUV measurements can also be used to infer the energy of precipitating electrons in aurorae. In this paper recent work in these areas will be reviewed. Requirements for future instrumentations will be discussed.

Introduction

The upper atmosphere and the *magnetosphere* (a complicated system controlled by the Earth's magnetic field filling a volume about a million times the volume of the solid Earth), forms a boundary between the Earth and space. Of this, only the lowest 5 km of the atmosphere is dense enough to sustain human life. Up to approximately 70 km altitude, the gas surrounding the Earth does not contain any significant concentration of ionic species. Above this altitude, the neutral gases are partially ionized by solar electromagnetic and corpuscular radiations, with some minor contributions from meteors. This spherical shell of ionized gases surrounding the Earth is called the *ionosphere.*

Several ionospheric layers have been discovered over the years. These layers result from differences in ion composition and vertical plasma transport mechanisms. The primary layers have been named D, E, F_1 and F_2, and range in altitude from approximately 70 to 100, 100 to 150, 150 to 250, and above 250 km, respectively. These regions have different density and temperature distributions, with the F_2 layer having the highest electron density at about 300 km. Long range radio communication is achieved by reflecting radio waves off the electrically conducting ionospheric layers.

The Department of Defense (DoD) operates various systems which depend critically on the state of these regions, especially the F_2 region. The F_2 layer is used extensively for High Frequency (HF) communications, over-the-horizon radars, global geopositioning satellites, etc.

The ionosphere and the magnetosphere are affected by disturbances in the Sun such as *solar flares.* Solar flares increase the relative amount of Ultraviolet (UV) radiation and charged particle flux that impinge upon the Earth. The *solar wind,* a continuous supersonic outflow of solar plasma, interacts with the Earth's magnetic field and results in a cigar-shaped cavity controlled by the Earth's magnetic field - the magnetosphere. Disturbances in the Sun such as solar flares have profound effects on the magnetosphere and the ionosphere. They result in *geomagnetic storms* which can change the structure of the ionosphere. The geomagnetic storms disrupt radio communications, surveillance equipments, electrical power distributions, and have been shown to accelerate corrosion in pipelines.

The most spectacular manifestation of the solar-terrestrial coupling is *aurora.* It is caused primarily by currents of high-energy magnetospheric electrons colliding with atmospheric gases, resulting in an atmospheric glow similar to that in neon lights. These charged particle showers in the polar regions are highly variable and change the atmospheric and ionospheric composition at timescales ranging from minutes to days.

The solar electromagnetic and corpuscular radiations govern the global plasma distribution of the F_2 layer, described in gross terms, by the height of the peak density (h_m), density at the peak (n_m), and the ion and electron temperatures. Since many of the DoD's Command, Control, Communication, and Intelligence (C^3I) operations depend critically on the instantaneous global state of the ionosphere, especially the F_2 layer, a need exists to monitor the global ionosphere on a routine basis.

Solar Extreme Ultraviolet (EUV) radiations are the key energy input in this complicated coupled system. From a remote sensing point of view, solar EUV emissions need to be monitored along with the neutral atmosphere and the ionosphere to provide a complete picture of the solar-terrestrial interactions. In addition, only a simultaneous monitoring of these three components can identify whether a transient response is a "natural phenomenon" or a man-made event. Lastly, the upper atmosphere, ionosphere and magnetosphere provide a natural laboratory for various atomic and plasma physics experiments in an environment difficult to simulate in a laboratory. Charged particle beam propagation experiments that have been conducted in the ionosphere simulate, in essence, a controlled auroral condition.

Measurement Techniques

Over the years various probing methods have been used from ground and space-based sensors. Traditionally, ionospheric measurements have used radio signals from ground-based ionosondes and radars. Ground-based sensors have the advantage of providing synoptic behavior of the ionosphere under various solar and geophysical conditions. They can also be modified easily to suit a given objective and can be repaired with equal ease. On the other hand, their measurements are confined to a fixed geographic region and cannot describe global phenomenology. Instruments sensitive to visible light have similarly been used to probe the neutral atmosphere and ionosphere. These optical instruments have a further limitation that they are dependent on the weather at the observation site. Moreover, these measurements suffer from ground albedo contamination.

Mass spectrometers and Langmuir probes aboard rockets and satellites have been used to measure the density and temperature of the neutral, ion and electron gases. Rocket-borne mass spectrometers and Langmuir probes provide altitude distribution but no geographical coverage. Even for satellite-based instruments, these *in situ* sensors provide information only along the satellite track.

Satellite borne sounders overcome some of these difficulties. While the ground-based ionosondes provide an accurate description of the ionosphere up to the altitude of the peak ionospheric plasma density, the topside sounders describe the conditions above the peak. However, the radio instruments operate as an active probe, which may be undesirable under certain situations. Moreover, they are typically bulky and require a large amount of electrical power.

In recent years, it has been shown that the Extreme and Far ultraviolet (EUV and FUV) spectral regions can be used for probing the neutral atmosphere and the ionosphere.[1,2] It has also been used in a limited sense to obtain the distribution of minor species in the plasmasphere.[3] The sensors used are typically much smaller than the radio experiments, do not require any cooling, and use only a fraction of the power required by most topside sounders. These EUV and FUV instruments have all the advantages of a visible-region sensor without the disadvantages discussed earlier. Ground albedo is negligible in the EUV and FUV, which is a major source of contamination for visible and infrared observations. They can provide global imagery as demonstrated vividly with the dramatic auroral images obtained by the Dynamics Explorer (DE), HILAT, Polar Bear and Viking satellites. EUV and FUV instruments have the added benefit of being able to monitor particle excited emissions such as auroral emissions under fully sunlit conditions as was shown with the above-mentioned imaging experiments. Furthermore, these sensors operate in a passive mode and hence are suitable for surveillance applications.

Recent interest in EUV and FUV remote sensing was sparked, in part, by the measurements of airglow and auroral emissions by the U. C. Berkeley EUV spectrometer aboard the STP78-1 satellite, and three Johns Hopkins University rocket instruments. The Berkeley instrument, for the first time, obtained EUV signatures of the neutral atmosphere and ionosphere under various geophysical conditions. Details of these and other measurements are discussed below.

Ionospheric Remote Sensing

At and above the peak of the F_2 region of the ionosphere, O^+ is by far the major positive ion and by charge neutrality requirements can be assumed to have the same abundance as the electron density. In the sunlit ionosphere, the O^+ ions resonantly scatter several allowed transitions produced by both photoionization and electron impact ionization of neutral oxygen atoms. It has been recently shown that the daytime ionospheric density and temperature can be estimated using the OII 834 Å emission.[4,2]

The potential of monitoring the nighttime ionosphere lies with the observation of EUV and FUV emissions produced by the radiative recombination of O^+ ions with ionospheric electrons:

$$O^+ + e \rightarrow O + h\nu$$

This process produces two bright EUV emission lines (at 1304 Å and 1356 Å) and a recombination continuum at 911 Å all of which have recently been observed spectroscopically from the U.S. Air Force STP78-1 satellite.[5]

These EUV and FUV emissions, when deconvolved using theoretical models of radiative transfer, solar EUV flux, atmospheric and ionospheric density profile models, can be used to infer the ion and neutral densities. In recent years, tremendous progress has been achieved in theoretical modelling of these emissions, so that we can now make accurate quantitative interpretation of the EUV measurements.[1,2] Progress has been aided by improved electron impact cross section measurements[6,7] as well as one satellite and several rocket observations .[8,5,1]

Daytime Ionospheric Remote Sensing

The EUV dayglow spectrum is quite rich in emission lines as shown in Figure 1. This spectrum was obtained by averaging a large number of individual spectra collected by the Berkeley EUV spectrometer on board the STP78-1 satellite.[9] Below 800 Å the spectrum is dominated by spectral lines of singly ionized oxygen. Because these spectra were obtained at 8 Å spectral resolution, it was not possible to positively identify all of the individual transitions. Hence, the excitation mechanism of several of these lines are somewhat uncertain. However, the OII 834 Å emission in the dayglow has been studied theoretically and its excitation mechanism and radiative transfer mechanism is relatively better understood.

The OII 834Å transition is a triplet emission with individual components at 834.462, 833.326 and 832.754Å. The OII 834Å photons are produced in the sunlit atmosphere by both photoionization and photo-electron impact ionization of neutral oxygen atoms.

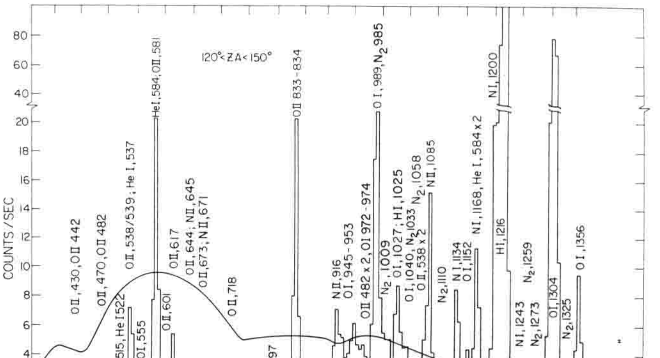

Figure 1. EUV dayglow spectrum at 600-km altitude obtained by averaging individual spectra taken while the spacecraft was between 50° N and 50° S, in the noon-midnight meridian in the period March 5-15, 1979, with the instrument pointed near nadir (zenith angle between 120° and 150°). The solid line labelled "100R" indicates instrument sensitivity in 100 R per wavelength bin. Representative 1 σ error bar is shown on the lower right-hand side of the diagram.

$$O + h\nu \rightarrow O^{+*} + e$$

$$O + e \rightarrow O^{+*} + e$$

$$O^{+*} \rightarrow O^{+} + h\nu_{834Å}$$

There is also a minor contribution from resonance scattering of sunlight, which can be neglected.

$$O^{+} + h\nu_{solar 834Å} \rightarrow O^{+} + h\nu_{834Å}$$

Once these photons are emitted, they are multiply scattered by the ground-state O^+ ions in the F_2 region. A computation of the volume production rates with and without the effects of multiple scattering are shown in Figure 2. This figure shows the initial (S_0) and the final (S) volume emission rates of the three multiplets as a function of altitude for typical atmospheric and ionospheric conditions.

Thus, a proper modelling of the OII 834 Å emission requires knowledge of the neutral oxygen density, the solar EUV flux, some parametric description of the O^+ density distribution, and models of photoelectron production rates and radiative transfer. Several radiative transfer models have been developed in recent years to analyze the OII 834 Å emissions. It has been shown that radiative transfer models using complete frequency redistribution (CFR) assumptions and plane parallel atmospheric layers are sufficient to describe the observed intensities under certain conditions.[4,10]

Previous analyses have treated the initial excitation rate as an adjustable parameter called the *g factor*. The g factor is the number of 834 Å photons produced per atomic oxygen atom per second. This was done due to the lack of laboratory cross section measurements of the two production mechanisms shown above. A Chapman layer has been used for O^+ density distribution. Such assumptions, although rather simplistic, have produced relatively good agreement between the observed and predicted intensities similar to that shown in Figure 3.

The success of these analyses indicates that a continuous monitoring of ionospheric weather may be possible through the observation of this transition. The U. S. Air Force has embarked on such a mission with the RAIDS experiment to be flown on a Tiros satellite.

There are several areas that need improvement before routine observations of the ionosphere becomes a reality. First, the theory of obtaining the densities from the intensities needs to be demonstrated with simultaneous measurements of several of the related parameters, such as ion density, solar flux, photoelectron flux, etc. Second, laboratory measurements of the photoionization and electron impact ionization cross sections need to be updated. Lastly, several ionospheric models predict the electron densities, all of which describe general features of the ionosphere, but they differ in describing the details. We are still far away from a generalized ionospheric model similar

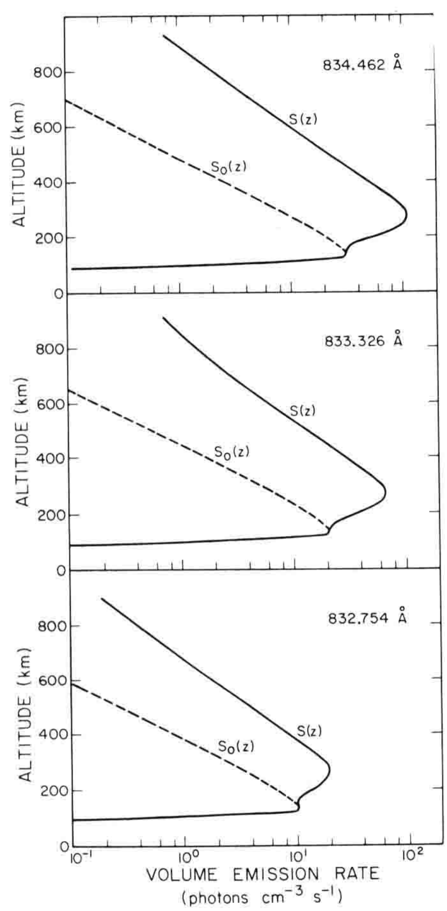

Figure 2. Initial and final emission rates (or source) functions are plotted as a function of altitude (z) for the three lines of the O^+ 834-Å triplet.

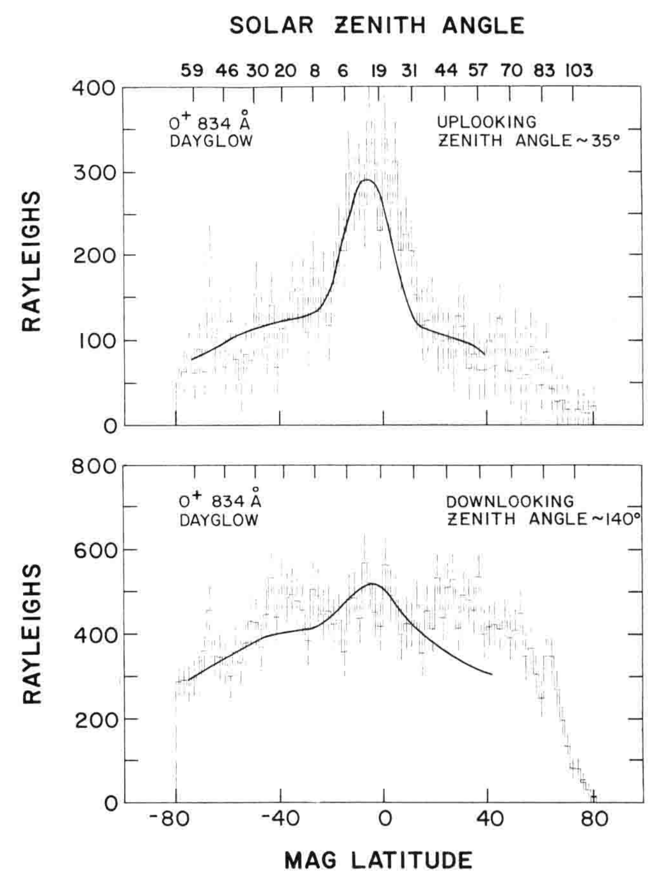

Figure 3. *Top*: O^+ 834-Å dayglow intensity observed at 600 km in a direction ~ 305 ° from zenith is plotted against geomagnetic latitude. One sigma error bar is also shown with each data point. The solar zenith angle corresponding to each latitude is indicated. The solid line represents best-fit model calculations. *Bottom*: Same as top for near nadir viewing direction (zenith angle ~ 140 °).

to the Mass Spectrometric and Incoherent Scatter (MSIS) model of the neutral atmosphere.

Small strides are being made in these areas. Cotton et al.[11] have used a comprehensive model ionosphere (the International Reference Ionosphere (IRI)), and atomic oxygen photoionization cross sections — obtained by combining total ionization cross sections[12] and branching ratios[13] — to compute expected intensities. These and other follow-up works will bring us closer to an accurate understanding of EUV emissions and their use for routine monitoring of the day time ionosphere.

Nighttime ionospheric monitoring

The nighttime ionosphere can be probed by the emissions produced by the recombination of O^+ ions with ambient electrons. These emissions have been imaged from the moon by a FUV camera[14] and also by the UV imager aboard the Dynamics Explorer satellite. Their spectral characteristics have been obtained by the Berkeley EUV spectrometer on board the STP78-1 satellite.[5] Although OI 989 Å emissions due to dielectronic recombination have also been measured by the same instrument,[15] the intensity is too low to use in remote sensing applications.

The radiative recombination mechanism produces two bright bands on either side of the magnetic dip equator as shown in Figure 4. The latitude distribution of these emissions correspond spatially with the equatorial fountain effect, also known as the *Appleton Anomaly*, which results from the enhanced electron density in this region. The principal features of the tropical ultraviolet airglow are the OI 1304 Å and 1356 Å lines and the recombination continuum at 911 Å. After geocoronal Lyman Alpha, these emissions are the dominant features in the EUV and FUV nightglow.[5]

It has been shown that if one assumes the ion distribution to be a Chapman Layer, then the nadir intensity for an optically thin transition resulting from radiative recombination of O^+ can be described as:[16]

$$I = \alpha n_m^2 \cdot H \cdot e$$

where, α is the radiative recombination coefficient, n_m is peak the electron density, H is the atomic oxygen scale height and e is the base for natural logarithms. Since the intensity depends on the square of the electron density, it is a very sensitive indicator of the peak density. For optically thick transitions, such as the OI 1304 Å line, multiple scattering radiative transfer models are required to predict the expected intensities.

Chakrabarti et al.[17] have shown that the zenith angle dependence of the intensities of these features can be explained with a Chapman layer distribution of O^+ density. In this parametric study the shape and magnitude of the spectral intensities were explained with reasonable values of the Chapman profile parameters. Simultaneous measurements of the emission intensities, ion and electron densities, temperatures, plus theoretical verifications using sophisticated radiative transfer models are needed to test the feasibility of remote sensing of the night time ionosphere.

An example of this kind of evaluation was presented by Link and Cogger.[18] These authors analyzed ground-based OI 6300 Å nightglow data using Arecibo radar measurements of ion temperature and electron density, along with recent revisions in laboratory rate coefficients. The authors noted an inverse correlation between the height of the F_2 peak and the 6300 Å line intensity. Furthermore, they have also observed a hysteresis effect when the observed intensities are plotted as a function of the measured height of the F_2 peak (see Figure 5). This dynamical effect was not reproduced in the intensities calculated using a steady-state model.

Tinsley et al.[19] have shown that the $\frac{\text{OI6300 Å}}{\text{OI1356 Å}}$ intensity ratio can be used to infer the altitude of the ionosphere. Gerard et al.[20] have shown that the same information can be obtained from the $\frac{\text{OI1304 Å}}{\text{OI1356 Å}}$ ratio. It will be important to verify these results with theoretical models and simultaneous ground-based radar and/or *in situ* mass spectroscopic measurements.

Although the intensities of the EUV and FUV features in the tropical airglow are quite high (~100 Rayleighs) the intensities outside these two bands are low (~20 Rayleighs). However, since the surrounding atmosphere is quite dark and there is no ground albedo, this level of signal can be detected with modern instrumentation. Furthermore, the variation of the intensities both within and outside the arcs can be used to study the dynamics and morphology of the nighttime ionosphere.

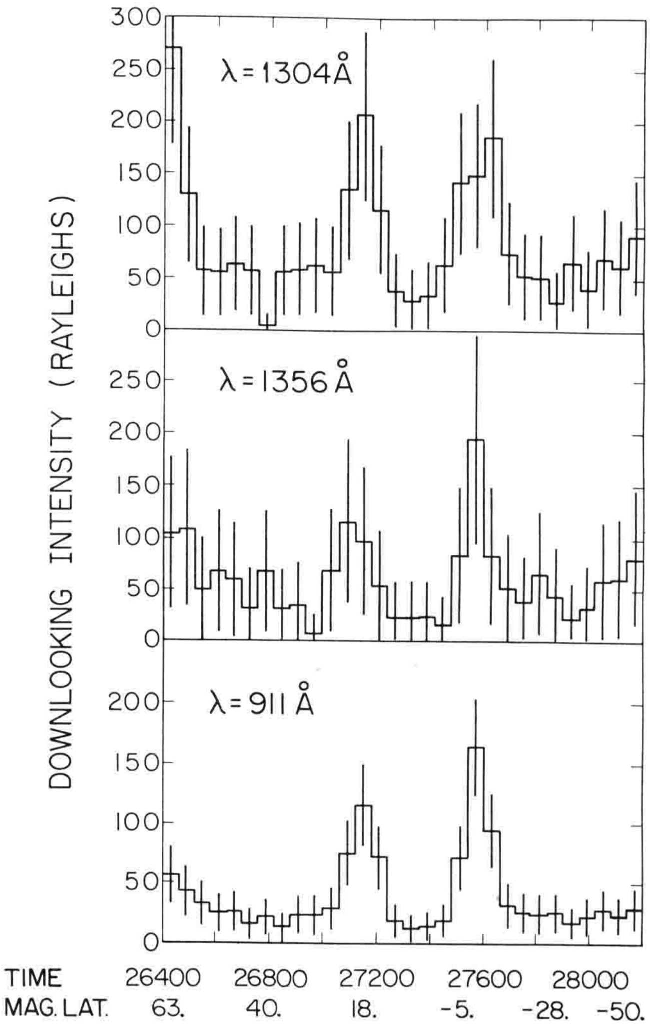

Figure 4. Latitude profiles of selected nightglow features for near nadir observation.

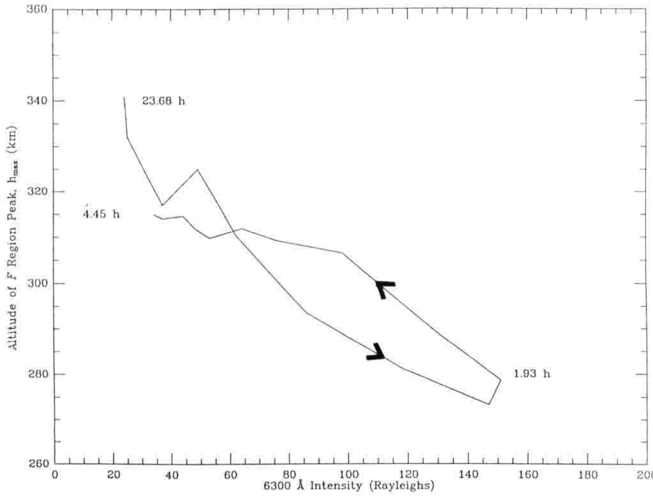

Figure 5. The altitude of the F region peak electron density, h_{max}, vs. the observed 6300-Å intensity. Local times of the observations are indicated in the plot.

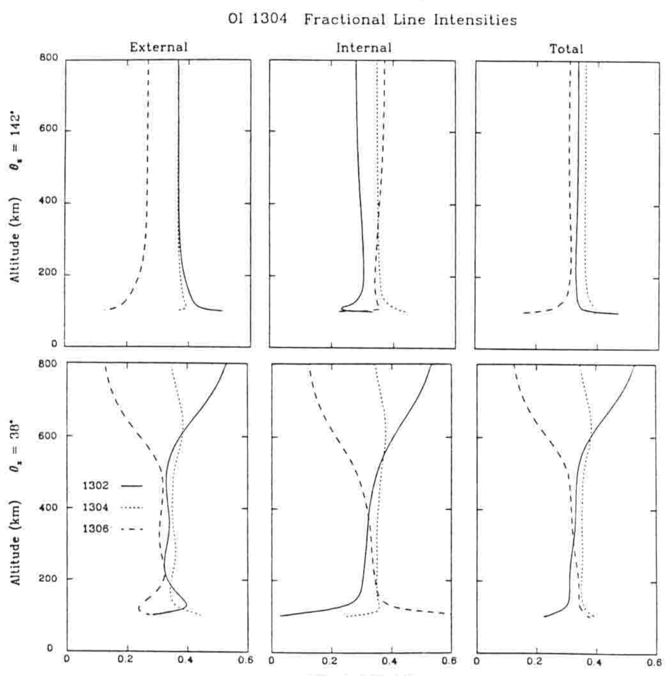

Figure 6. Fractional contributions of the 1302 (solid line), 1304 (dotted line), and 1306 (dashed line) lines to the total 1304-Å triplet intensity for downlooking (142°, top row) and uplooking (38°, bottom row) cases. *Left*: external (solar source). *Center*: internal (photoelectron source). *Right*: total.

Neutral Atmosphere

More progress has been made in the remote sensing of the neutral atmosphere than the ionosphere. Link et al.[1] have analyzed three EUV spectral features of atomic oxygen measured as a function of latitude at local noon by the STP78-1 satellite; they have obtained excellent agreement with the data using the most recent laboratory measurements of excitation cross sections. The authors have also used simultaneous observations of density and temperature obtained by the Atmospheric Explorer (AE)-E satellite.

The three features studied were the OI transitions at 989 Å, 1304 Å and 1356 Å. These emissions have different excitation and radiative transfer properties. While the 989 Å and 1356 Å transitions are produced only by photoelectron impact in the atmosphere, the 1304 Å emission has a strong contribution from resonantly scattered solar 1304 Å emission. The 989 Å and 1304 Å emissions are very optically thick in the Earth's atmosphere. Once produced, these photons are typically scattered $10^3 - 10^4$ times by atmospheric O atoms, before escaping the medium. However, the 1356 Å emission results from a dipole-forbidden transition, and hence is optically thin. These various excitation and radiative properties can be used to determine thermospheric oxygen densities in a self-consistent manner.

These OI emissions have been observed from two rocket-borne spectrometers.[8] Although the authors[8] were able to explain these photoelectron-excited emissions with reasonable atmospheric and solar conditions, the electron impact cross sections have recently been revised downward by a factor of 3 – 20. Link et al.[21] were able to explain these rocket measurements with the same parameters as used for analyzing the STP78-1 data. These successes indicate that the atomic oxygen density can be inferred from the observations of these transitions. However, a few details must be verified before an unqualified confident determination can be made of the O density distribution. A multi-instrument measurement of several parameters such as the solar flux, O density, photoelectron flux and the EUV/FUV intensities, will convincingly prove the validity of this technique.

Two future experiments are aimed towards this goal. A three-spectrometer rocket experiment is planned by the Berkeley group to simultaneously measure the solar flux in the 250-1400 Å range, and the dayglow in the 980-1040 Å and 1300-1360 Å ranges.[22] While the solar spectrometer require only a resolution of ~10 Å, the airglow will be measured at a resolution of 0.5 Å. Such spectral resolution will separate the individual transitions within the 989 Å, 1304 Å and 1356 Å multiplets and verify their altitude dependence as predicted by Link et al.[1] (See Figure 6.) The second experiment will be conducted from the joint U.S.-German-Italian spacecraft San Marco. This satellite will carry a spectrometer which will measure the airglow and solar spectra in a wide spectral region from EUV to near infrared.[23]

The 1304 Å feature in the tropical airglow is optically thick. These photons are multiply scattered by the thermospheric O atoms. The nighttime O density can therefore be inferred from the 1304 Å emission. Under certain conditions, the photoelectrons produced in the sunlit hemisphere travel along the Earth's magnetic field lines to the dark side and excite the atmospheric species. Such mechanism has been observed to produce as much as 100 Rayleighs of 1304 Å line[24] and can be used to probe the night side atmosphere. Emissions from other species such as N_2 and transitions of atomic oxygen at 1356 Å and 989 Å should also be produced by this mechanism.

Molecular nitrogen is the next important neutral species in the upper atmosphere. Observation of the Lyman Birge Hopfield (LBH) band system has been used to determine the N_2 densities and validate photoelectron flux models.[8,21]

Polar Atmosphere and Ionosphere

In the polar region, an additional source of energy input must be taken into account — the precipitating particles. Auroral electrons and protons have different energy characteristics and the emissions produced by them show different spectral and altitude profiles.[25] EUV and FUV wavelength regions are important in probing auroral emissions. Recent imagery experiments have shown spectacular images of the polar aurora in the FUV. These images vividly demonstrate that the aurora can be optically investigated even under fully sunlit conditions. Such observations are not possible in the visible or near infrared regions, where most of the optical auroral research has taken place. A number of spectroscopic measurements of different types of auroral conditions have recently been reported in the literature.[25,26] These observations have extended auroral observations to ~ 400 Å and have revealed a large number of previously unobserved transitions and phenomena.

Theoretical analysis of these emissions require additional modelling of photo-electron and auroral transport.[27,28,29] Accurate estimation of the particle energy and flux require the use of these models. For the sunlit aurora these computations must be carried out in conjunction with the normal dayglow computations.[30]

Simple estimates of incoming particle energy can be obtained by determining the altitude of the emission peak through examination of the intensity ratios of different spectral lines. The $\frac{\text{OI 989 Å}}{\text{OI 1027 Å}}$ ratio is one such candidate. They both have similar excitation cross sections and similar volume emission profiles. However, O_2 molecules have different absorption cross sections for these two emissions, and if the emissions are peaked deeper in the atmosphere, then the ratio will be lower, due to preferential absorption of the 989 Å multiplet.

The auroral atmosphere is an ideal candidate for experimenting with remote sensing concepts. It provides a natural laboratory for many physical, chemical and dynamic phenomena with highly varying spatial and temporal morphologies. Furthermore, aurora provide naturally occurring events that mimic many of the events of interest to the DoD.

Instrumentation issues

One of the reasons for the lack of experimental work in EUV remote sensing of the upper atmosphere is the difficulty in sensor technology. For instance, no window materials can be used in the EUV region. Furthermore, due to the observational difficulties, most of the research on materials and technology had to wait until rockets and satellites became available for experimentation.

These wavelengths have the advantage that for a given required spatial resolution, they provide diffraction limited performance using smaller optics than the optical, infrared or radio counterparts. Power requirements for these instruments are minimal. These characteristics make them ideally suited for space applications, where weight, size and power are precious.

In the past years the detector technology has advanced tremendously. Microchannel Plate (MCP) and Charged Coupled Devices (CCDs) have been used routinely in many space instrumentations.[31–35] These detectors can provide two-dimensional electronic imaging capabilities. The MCP based detectors have the added advantage that they do not require any cooling, cryogenic or otherwise, and hence may be preferable for space-based applications. The CCDs typically have large dynamic range, but for fast varying phenomena MCPs are ideal. Different optical coating materials have been evaluated for their suitability in various wavelength regions. Among these Gold, Magnesium Fluoride, Iridium, Osmium and Platinum have been used in several space experiments. Silicon Carbide shows high promise for use as a possible optical coating and may increase the reflectivity over most other materials by almost a factor of two in the EUV wavelength range.[33] Similar experimentations have been conducted with photocathode materials for use in the detectors. Magnesium Fluoride, Cesium Iodide and Potassium Bromide and other halides are being used routinely.[34,35] Unlike the photocathodes used in the visible region, these materials need not be cooled to lower the inherent dark noise background. These and other advances offer the tantalizing possibility of routine monitoring of the atmosphere and the ionosphere using long-lived space- and ground-based passive sensors.

Summary

Highlights of recent theoretical and experimental advances in the remote sensing of the ionosphere and atmosphere have been described. It has been shown that selected EUV and FUV spectral lines may be used using passive measurement techniques to describe the instantaneous state of the ionosphere and the upper atmosphere. Significant progress has been made in various technological areas so that we can begin to exploit this new window to space for various DoD and civilian applications.

Acknowledgements

This work was funded by NSF funds ATM 85-15008 and ATM 84-20573 and US Army DAAG29-85-K-0248.

References

1. R. Link, S. Chakrabarti, G.R. Gladstone, J.C. McConnell, "An Analysis of Satellite Observations of the OI EUV Dayglow," *J. Geophys. Res.*, in press, 1987.
2. R.P. McCoy, D.E. Anderson, Jr., S. Chakrabarti, "F_2 Region ion densities from analysis of O^+ 834-Å airglow: A parametric study and comparisons with satellite data," *J. Geophys. Res.*, **90**, 12,257, 1985.
3. S. Chakrabarti, F. Paresce, S. Boywer, Y.T. Chiu, A. Aikin, "Plasmaspheric helium ion distribution from satellite observations of He II 304-Å," *Geophys. Res. Letters*, **9**, 151, 1982.
4. S. Kumar, S. Chakrabarti, F. Paresce, S. Bowyer, "The O^+ 834-Å Dayglow: Satellite Observations and Interpretation with a Radiation Transfer Model," *J. Geophys. Res.*, **88**, 9271, 1983.
5. S. Chakrabarti, R.A. Kimble, S. Bowyer, "Spectroscopy of the EUV (350-1400 Å) Nightglow," *J. Geophys. Res.*, **89**, A7, 1984.
6. E.C. Zipf, P.W. Erdman, "Electron impact excitation of atomic oxygen: Revised cross sections," *J. Geophys. Res.*, **90**, 11087, 1985.
7. S.O. Vaughan, J.P. Doering, "Absolute differential and integral electron excitation cross sections for atomic oxygen, 3, The $(^3P - {}^3D^o)$ transition (989 Å) from 20 to 200 eV with improved values for the $(^3P - {}^3S^o)$ transition (1304 Å)," *J. Geophys. Res.*, **92**, 7749, 1987.
8. R.R. Meier, R.R. Conway, D.E. Anderson, Jr., P.D. Feldman, R.W. Eastes, E.P. Gentieu, A.B. Christensen, "The ultraviolet dayglow at solar maximum, 3, Photoelectron-excited emissions of N_2 and O," *J. Geophys. Res.*, **90**, 6608, 1985.
9. S. Bowyer, R. Kimble, F. Paresce, M. Lampton, G. Penegor, "A Continuous Readout Extreme Ultraviolet Airglow Spectrometer," *Appl. Opt.*, **20**, 477, 1981.
10. D.E. Anderson, Jr., R.R. Meier, "The OII 834Å Dayglow: A General Model for Excitation Rate and Intensity Calculations," *Planet. Space Sci.*, **33**, 1179, 1985.
11. D.M. Cotton, R. Link, G.R. Gladstone, S. Chakrabarti, "An analysis of the OII 834Å dayglow," *EOS Trans. AGU*, **68**, 1397, 1987.
12. J.A.R. Samson, P.N. Pareek, "Absolute photoionization cross sections of atomic oxygen," *Phys. Rev. A*, **31**, 1470, 1985.